KINETICS OF CHEMICAL REACTIONS OF METHANE IN THE FLOWING AFTERGLOW OF A DINITROGEN MICROWAVE PLASMA

J.-C. Legrand (*), A.M. Diamy (*), R. Hrach (°), and V. Hrachová (°)

(*): Laboratoire de Chimie Générale et de Chimie des Surfaces, CNRS URA 1428, Univ. Pierre et Marie Curie, Case 196, 4 place Jussieu, 75252 Paris Cedex 05, France.
(°) Department of Electronics and Vacuum Physics, Faculty of Mathematics and Physics, Charles University, V Holešovičkách 2, 18000 Prague, Czech Republic.

The reaction of methane in the afterglow is studied by combination of computer experiments and direct measurements. Methane conversion is mainly initiated by active neutral species. The first step is the dissociation of methane in CH_x and H radicals. The main products obtained are C_2H_6, C_2H_4, C_2H_2 along with HCN and H_2. For simulation, the model is based on a macroscopic kinetic approach concerning 24 species and 58 reactions. As a result, the steady state concentrations of stable products are derived

1) Introduction

The methane decomposition reaction with discharged dinitrogen is an important aim of investigation for chemical applications as detoxification [1], atmospheric chemistry of Titan [2], metallurgy [3], synthesis [4]... We have analyzed products obtained from conversion of methane introduced in the afterglow of a dinitrogen plasma and proposed a kinetic scheme that could explain the results [5]; this study is an attempt of modeling the results to derive the steady-state concentrations of stable products when methane is introduced in the post-discharge.

2) Experimental set up

The experimental set up is shown in figure 1. A microwave generator (Thomson-CSF, 2.45 GHz, adjustable power up to 1.5 kW) is connected to a rectangular waveguide cavity of about one meter length. Resonance is obtained by adjusting the position of a sliding short located at the end of the cavity. Stationary electromagnetic waves produce a plasma in a cylindrical reactor crossing the cavity. The reactor is made of fused silica and its inner diameter is 2.8 cm (o.d. = 3 cm). Methane is introduced into the plasma gas by means of five ports distributed all around the reactor. Another port is used to measure the pressure P or to measure electron characteristics with a Langmuir double probe [6]. The pressure is measured by means of a baratron (MKS 122A) and the gas flow rates F (in STP conditions, i.e. 298 K and 1 bar) by means of mass flowmeters (Alfagaz RDM 280).

Chemical analysis is performed by gas chromatography (Girdel 3000 with a Thermal Conductivity Detector). Dinitrogen, methane, and dihydrogen are separated by a silicagel column (6.40 m long); ethane, ethylene, and acetylene are separated by a shorter column (1.80 m long). Traces of propane and butane are also detected. Nitriles are trapped by silicagel columns so they cannot be analyzed.

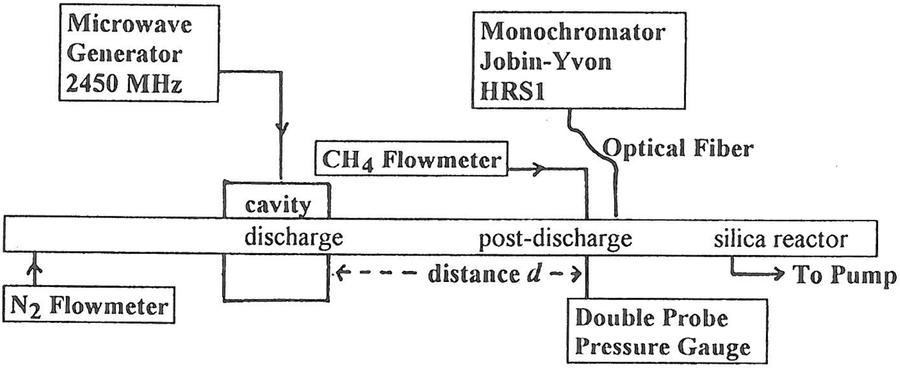

Fig.1: Experimental set-up.

3) Experimental results

Figures 2 and 3 show gas temperature, electron temperature, electron density methane conversion (α), N_2 decay (γ), and C_2 hydrocarbon yield versus distance of methane introduction in the post-discharge for the following experimental conditions: pressure = 13 mbar, N_2 flowrate = 200 ml STP/min, CH_4 flowrate = 150 ml STP/min, incident power = 370 watts. Computations are carried out to try to explain the results.

4) Computations

4-a) Mechanism :

We introduce methane in the post-discharge, so charged species can have influence only for the shorter distances (Fig. 2). Hot electrons can dissociate CH_4 by reactions 1 to 4 in the mechanism. The ion concentration is about 1.10^{12} part/mL according to electroneutrality (Fig. 2). Ion-neutral reaction can have fast rate constants but, in this first computation, we do not take these reactions in account because amount of ions is very low.

The kinetic scheme taken into account includes the 58 following reactions:

1	$CH_4 + e$	--->	$CH_3 + H + e$	$k_1 = a.k_0 = f(T_e)$
2	$CH_4 + e$	--->	$CH_2 + 2H + e$	$k_2 = b.k_0 = f(T_e)$
3	$CH_4 + e$	--->	$CH + 3H + e$	$k_3 = c.k_0 = f(T_e)$
4	$CH_4 + e$	--->	$C + 4H + e$	$k_4 = d.k_0 = f(T_e)$
5	$CH_4 + N_2$ (A,v)	--->	products ($CH_3 + H + N_2$)	$1.5x10^{-12}$ (v=1)
6	$CH_3 + CH_3$	--->	C_2H_6	$4.0x10^{-10}.T^{-0.4}$
7	$CH_2 + CH_2$	--->	C_2H_4	$1.7x 10^{-12}$
8	$CH_3 + CH_2$	--->	$C_2H_4 + H$	$7.0x10^{-11}$
9	$CH_4 + CH$	--->	$C_2H_4 + H$	$5.0x10^{-11}.exp(+200/T)$
10	$C_2H_5 + CH_3$	--->	$C_2H_4 + CH_4$	$1.9x10^{-12}$
11	$C_2H_5 + C_2H_5$	--->	$C_2H_6 + C_2H_4$	$2.4x10^{-12}$
12	$C_2H_6 + N_2$ (A,v)	--->	$C_2H_5 + H + N_2$	$3.6x10^{-12}$(v=1)
13	$C_2H_6 + H$	--->	$C_2H_5 + H_2$	$2.4x10^{-15}xT^{1.5}.exp(-3730/T)$
14	$CH_3 + CH_3$	--->	$C_2H_5 + H$	$1.3x10^{-9}.exp(-13\ 275/T)$
15	$C_2H_6 + CH_3$	--->	$C_2H_5 + CH_4$	$2.5x10^{-31}xT^{6}.exp(-3730/T)$
16	$CH_2 + CH_2$	--->	$C_2H_2 + 2H$	$2.0x10^{-10}.exp(-400/T)x0.9$
16bis	$CH_2 + CH_2$	--->	$C_2H_2 + H_2$	$2.0x10^{-10}.exp(-400/T)x0.1$
17	$CH + CH$	--->	C_2H_2	$2.0x10^{-10}$
18	$CH_3 + C$	--->	$C_2H_2 + H$	$8.3x10^{-11}$
19	$CH_2 + CH$	--->	$C_2H_2 + H$	$6.6x10^{-11}$
20	$CH_3 + N$	--->	$HCN + H_2$	$1.4x10^{-11}$
21	$CH_2 + N$	--->	$HCN + H$	$8.3x10^{-11}$
22	$CH_4 + CN$	--->	$HCN + CH_3$	$7.0x10^{-13}(T/293)^{2.3}.exp(+16/T)$
23	$CH_4 + H$	--->	$H_2 + CH_3$	$2.2x10^{-20}xT^{3.0}.exp(-4045/T)$
24	$C_2H_5 + CH_3$	--->	C_3H_8	$4.7x10^{-11}$
25	$C_2H_5 + C_2H_5$	--->	C_4H_{10}	$1.9x10^{-11}$
26	$CH_3 + N$	--->	$H_2CN + H$	$1.3x10^{-10}$
27	$H_2CN + N$	--->	$HCN + NH$	$6.7x10^{-11}$
28	$C + N_2$	--->	$CN + N$	$1.1x10^{-10}.exp(-23\ 000/T)$
29	$CH + N$	--->	$CN + H$	$2.1x10^{-11}$
30	$CH_2 + N$	--->	$CN + H_2$	$1.6x10^{-11}$
31	$CH_4 + CH_3$	--->	$C_2H_5 + H_2$	$1.7x10^{-11}.exp(-11\ 500/T)$
32	$CH_4 + CH_2$	--->	$CH_3 + CH_3$	$7.1x10^{-12}.exp(-5020/T)$
33	$CH_4 + C_2H_3$	--->	$CH_3 + C_2H_4$	$2.4x10^{-24}xT^{4}.exp(-2754/T)$
34	$CH_2 + C$	--->	$C_2H + H$	$8.3x10^{-11}$
35	$C_2H_2 + H$	--->	$C_2H + H_2$	$1x10^{-10}.exp(-14000/T)$
36	$CH_3 + CH$	--->	$C_2H_3 + H$	$5x10^{-11}$
37	$C_2H_2 + H + N_2$	--->	$C_2H_3 + N_2$	$1x10^{-10}.exp(-14000/T)$
38	$H + H + N_2$	--->	$H_2 + N_2$	$1.5x10^{-29} / T^{1.3}$
39	$N + N + N_2$	--->	$2 N_2$	$8.3x10^{-34}.exp(+500/T)$
40	H + wall	--->	$0.5 H_2$	$1.9x10^{-1}.exp(-4930/T)$
41	N + wall	--->	$0.5 N_2$	$1.9x10^{-3}.exp(-1680/T)$
42	$CH_4 + N(*)$	--->	$CH_3 + NH$	$1.5x10^{-12}$

43	$CH_4 + C_2H \longrightarrow C_2H_2 + CH_3$	2.0×10^{-12}
44	$CH + N_2 \longrightarrow HCN + N$	$1.7 \times 10^{-14} \cdot \exp(975/T)$
45	$CH_3 + e \longrightarrow CH_2 + H + e$	$k = f(T_e)$
46	$CH_2 + e \longrightarrow CH + H + e$	$k = f(T_e)$
47	$CH + e \longrightarrow C + H + e$	$k = f(T_e)$
48	$C_2H_3 + H \longrightarrow C_2H_2 + H_2$	2×10^{-11}
49	$C_2H_3 + CH_3 \longrightarrow C_2H_2 + CH_4$	6.5×10^{-13}
50	$CH_2 + C_2H \longrightarrow C_2H_2 + CH$	3.0×10^{-11}
51	$CH_2 + C_2H_3 \longrightarrow C_2H_2 + CH_3$	3.0×10^{-11}
52	$C_2H_5 + H \longrightarrow C_2H_6$	6.0×10^{-11}
53	$C_2H_5 + C_2H_3 \longrightarrow C_2H_6 + C_2H_2$	8.0×10^{-13}
54	$C_2H_5 + C_2H_3 \longrightarrow C_2H_4 + C_2H_4$	8.0×10^{-13}
55	$C_2H_5 + C_2H \longrightarrow C_2H_4 + C_2H_2$	3.0×10^{-12}
55	$C_2H_6 + C_2H \longrightarrow C_2H_2 + C_2H_5$	6.0×10^{-12}
57	$CH_3 + H + N_2 \longrightarrow CH_4 + N_2$	$6.10^{-29}.(T/300)^{-1.8}$

Rate constants are taken from reference [5]

4-b) Integration of the ordinary differential equations

For simulation, the model is based on a macroscopic kinetic approach concerning 24 species and 58 reactions. The integration of the stiff system is performed using a fourth order Rosenbrock method with the Kaps-Rentrop algorithm or using a semi-implicit extrapolation method (Bader-Deuflhard method) [7]. As a result, the steady state concentrations of stable products are derived.

5) Results

5-a) Influence of N atom concentration

Computations have been done with reactions 1 to 44 at a distance *d* = 1.9 cm where charged species are not present. N atom density was changed from 0.5 to 5 p. cent (Fig. 4). Excited dinitrogen molecules were created during the kinetic time. We observe a great influence of N atom concentration on the ratio C_2H_6 / HCN. The experimental data for C_2H_6 correspond to a density of about 2.3 % of N atoms.

5-b) Influence of electrons

When we are near the end of the discharge (*d* = 0.9 cm), charged species are present. The total rate constant k_0 for the reaction $CH_4 + e \longrightarrow$ products is given in the literature [5], but the channels for reactions 1 to 4 are not known. We change the proportions a, b, c, and d in the distribution $k_0 = (k_1 + k_2 + k_3 + k_4)$. It appears that electrons have a little influence in the mechanism, so the most important way of decay for methane is reactions with excited dinitrogen, i.e., $N_2(A,v)$ and $N_2(X,v>18)$.

5-c) Influence of $N_2(^*)$ concentration

Figure 5 shows emission intensity of several bands of N_2 spectrum [$N_2(B,11 \longrightarrow A,7)$, $N_2(C,0 \longrightarrow B,2)$ and $N_2^+(B,0 \longrightarrow X,0)$] observed in the post-discharge for pure dinitrogen and for the mixture of dinitrogen with methane. The $N_2(B,11 \longrightarrow A,7)$ band which is the signature of N atom recombination disappears in the mixture, indicating rapid reactions of N with CH_x radicals. The $N_2^+(B,0\text{---}>X,0)$ band disappears too, as yet observed [6], indicating the absence of excited ions. The $N_2(C,0\text{---}>B,2)$ band is increased; this result shows the creation of excited molecules $N_2(A)$ and $N_2(X,v)$ as shown in another paper of this conference [8]. Concentration of excited dinitrogen $N_2(*)$ has been changed in different manners in computations : (a) only decay from a maximum value (t = 0), (b) creation along the post-discharge. The creation of excited dinitrogen in the post-discharge is due to vibrational/vibrational transfer between dinitrogen molecules when translational temperature of gas is going down.

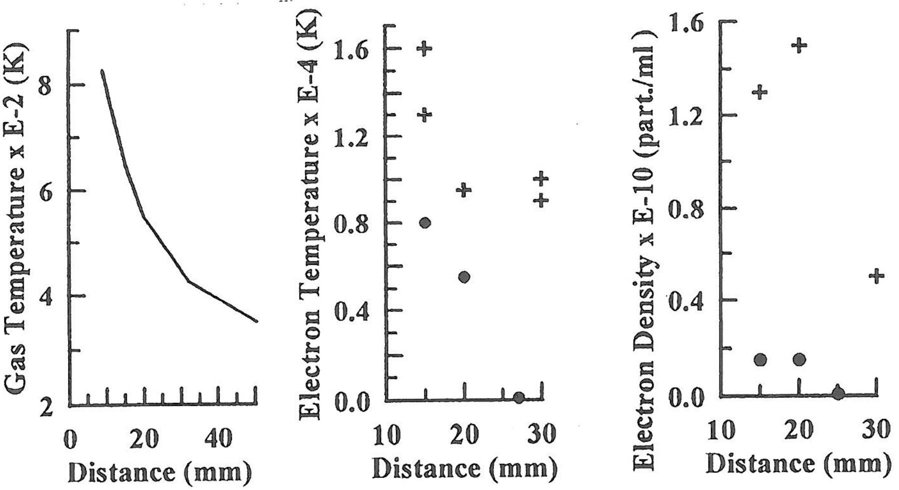

Fig. 2 : Gas temperature, electron temperature and electron density versus distance.
+ : pure N_2; ● : N_2/CH_4.

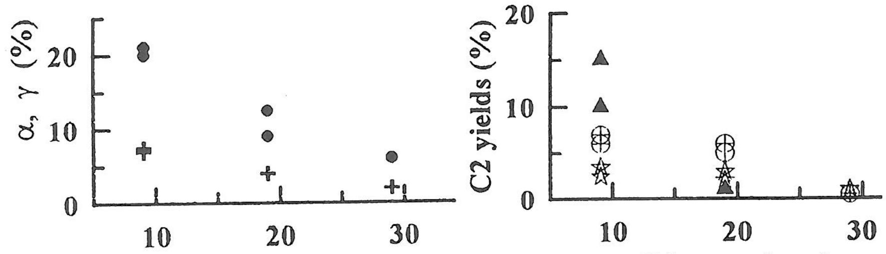

Fig. 3 : Methane conversion α (●), N_2 decay γ (+), and C_2 hydrocarbon (▲: C_2H_2; ⊕ : C_2H_6, ☆ : C_2H_4) yield versus distance of methane introduction.

These preliminary results show the great influence of excited metastable molecules of dinitrogen in the methane conversion and the role of nitrogen atoms in the relative proportions of C_2H_6 and HCN when methane is introduced downstream the decay of electrons. When electrons are present, the mechanism used does not account for the high yield of acetylene measured, probably, because ethane and ethylene must also be destroyed by electrons to give CH and C which are the main radicals leading to C_2H_2.

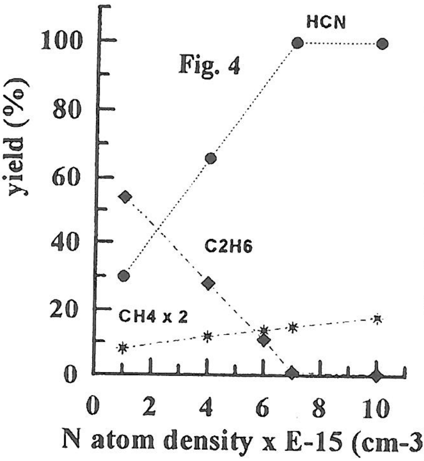

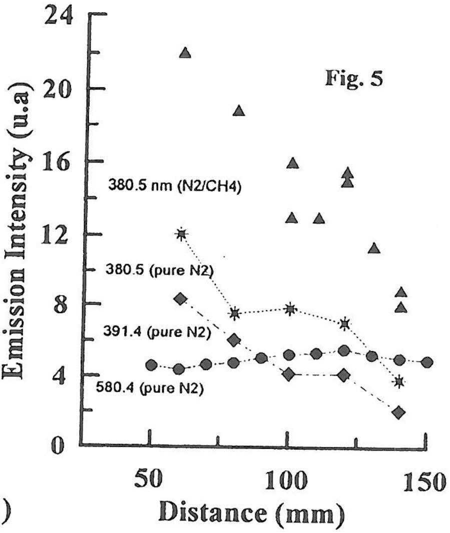

Fig. 4 : Influence of N atom concentration on the ratio C_2H_6 / HCN (computation).

Fig. 5 : Emission intensity of [N_2(B,11--->A,7): 580.4 nm, N_2(C,0--->B,2): 380.5 nm, and N_2^+(B,0--->X,0): 391.4 nm] observed in the post-discharge for pure dinitrogen and for the mixture of dinitrogen with methane versus distance d.

References:

[1] M.E. Fraser, D.A. Fee and R.S. Sheinson, *Plasma Chem. and Plasma Process.*, 5, 163 (1985).

[2] W.R. Thompson, T.J. Henry, J.M. Schwartz, B.N. Khare and C. Sagan, *Icarus*, **90**, 57 (1991).

[3] A. Ricard, J.Oseguera, L. Falk, H. Michel and M. Gantois, *I.E.E.E. Trans. Plasma Sci.*, **18**, 940 (1990).

[4] D. Rapakoulias and J. Amouroux, *Revue Phys. Appl.*, 15 , 1251 (1980).

[5] A Oumghar, J.C. Legrand, A.M. Diamy, N. Turillon and R.I.Ben-Aim, *Plasma Chem. and Plasma Process.*, 14, 229 (1994).

[6] A.M. Diamy, J.C. Legrand and V. Hrachova, *J. Phys. III Fr.*, 5, 435 (1995).

[7] W.H. Press, B.P. Flannery, S.A. Teukolsky and W.T. Vetterling, in *Numerical Recipes in Fortran*, Cambridge Univ. Press (Sd Ed) p 727 (1992).

[8] J. Al Andari, A.M. Diamy, L; Hochard, J.C. Legrand and A. Ricard, *12th Intern. Symp. on Plasma Chemistry* (Minneapolis) (1995).

Acknowledgments: the financial support of the European Community (COPERNICUS N° CIPA-CT94-0183) for this work is gratefully acknowledged.

We wish to thank Mmes J. Al Andari and N. Turillon for technical support.